

Synthesis, Structural Characterisation and Biological Activity of New Mannich Compounds Derived from Cyclohexanone Moiety

Alaa Mohammed Etheb¹, Mohamad J. Al-Jeboori^{2*}

^{1,2}Department of Chemistry, College of Education for Pure Science (Ibn Al-Haitham), University of Baghdad, Adhamiyah, Baghdad, Iraq
Email: mohamad.al-jeboori@ihcoedu.uobaghdad.edu.iq

Abstract

The formation and structural investigation of three new Mannich bases are reported. The synthesis of these compounds was accomplished via a multicomponent one-pot reaction using CaCl₂ as a catalyst. The reaction of the benzaldehyde, *m*-bromoaniline and cyclohexanone or 4-methylcyclohexanone resulted in the formation of L1 and L3, respectively. The synthesis of L2 was achieved by mixing benzaldehyde, *o*-bromoaniline and cyclohexanone. The isolated compounds were characterised using a range of analytical and spectroscopic techniques. These include; NMR (¹H and ¹³C-NMR), ESMS, FTIR, electronic spectroscopy, microanalyses and melting points. The NMR data for L1 and L2 indicated the presence of one isomer in solutions, on the NMR time scale. However, the NMR analyses for L3 confirmed the presence of two isomers in the solution. The title compounds are potential materials that may use as complexation agents for metal ions and/or be used as precursors in the formation of new organic compounds including a new type of ligands. The biological activity of the prepared compounds against bacterial and fungi species was also investigated.

Keywords: Mannich bases; One-pot approach; Multicomponent reaction; Cyclohexanone moiety; Structural study; Biological activity.

1. Introduction

The one-pot approach is a convenient route for the formation of Mannich compounds, which is based on the mixing of three-component materials in one vessel. Mannich reaction is a versatile and remarkable route of reaction that has a role in the development of synthetic chemistry, including organic and medicinal chemistry [1]. One interesting aspect of Mannich chemistry is the formation of new organic compounds including natural products [2,3]. The synthetic method to generate the required Mannich compounds is a straightforward multicomponent reaction that is achieved in the presence of a catalyst [4]. This approach represents a key direction in the implementation of the green chemistry approach [5]. Mannich compounds have applications in the field of medicinal chemistry, which include the formation of compounds to be evaluated as antimalarial, antitumour, antimicrobial, antitubercular, antiinflammatory and anticonvulsant agents [1,6]. More, Mannich bases have shown the ability to be used as complexation agents. This is based on the involvement of the carbonyl oxygen moiety of the cyclohexanone segment and the nitrogen atom of the secondary amine in the coordination with the metal centres [7,8]. Further, compounds derived from the Mannich reaction may be used as precursors to fabricate a variety of interesting ligands [6,9-12]. As part of our continuing effort to explore the formation of new organic compounds derived from the Mannich

approach, this work intends to examine the synthesis and structural characterisation of new Mannich-bases derived from the cyclohexanone moiety. These compounds may use as complexation agents and/or as precursors to prepare new ligands. Further, the biological activity of the prepared compounds is explored. The activity was compared with the approved antibiotics, Ceftriaxone and Fluconazole, which indicated these compounds are potential antifungal candidates (as they showed higher activity, compared with Fluconazole).

2. Experimental

Materials and Methods

The commercially purchased chemicals in this work were used without further purification. The solvents used in experiments were analytical-reagent grade. The ¹H- and ¹³C-NMR spectra were measured in DMSO-d₆ solutions on the Bruker 400 MHz instrument using TMS as an internal standard. The electrospray mass spectra (ESMS) were recorded using Sciex Esi mass spectrometer. The FT-IR spectra were recorded as KBr discs in the range 4000-400cm⁻¹ using an FTIR-600 FT-IR spectrometer. The electronic spectra were recorded using a Shimadzu UV-Vis 1800 in the range 11000-200nm using quartz cells of (1.0) cm length with a concentration of 10⁻³ mol L⁻¹ of samples in DMSO at room temperature. Elements analysis (C, H and N) were carried out on a Heraeus instrument (Vario EL). Melting points were determined on an electrothermal Stuart apparatus, model SMP40.

Synthesis

The synthesis of L1-L3 was accomplished using a published method [4,7,8] and as follows:

Synthesis of L1

In a 100ml round-bottomed flask charged with anhydrous CaCl₂ (1.1g, 10mmol) dissolved in 15ml of EtOH with 3-5 drops of HCl (36%), was added with stirring benzaldehyde (1ml, 10mmol) and *m*-bromoaniline (1.1ml, 10mmol). The mixture was kept in an ice bath, and then cyclohexanone (1ml, 10mmol) was added slowly. The resultant mixture was heated for two h at 50-60°C and then stirred for an hour at room temperature, during which time a solid was formed. The desired product was filtered off, washed with distilled water (50ml) and EtOH (60ml), and then air-dried. Yield: 1.80g (51%), m.p = 134-136°C. Elemental analysis: (C.H.N) Found, (Calc. %); C=63.41 (63.70), H=5.63 (5.69), N=3.78 (3.91). FT-IR (KBr) cm⁻¹, 3382 ν(N-H), 1695 ν(C=O), 1602 cm⁻¹ ν(C=C)_{aromatic} and 1512 δ(N-H). The ¹H-NMR spectrum (400MHz, DMSO-d₆) of L1 showed peaks at δ_H (ppm); 7.41-7.40 (2H, d, C-H_{15,15}-, J = 7.24 Hz), 7.31-7.27(2H, t, C-H_{16,16}-, J = 7.4, 7.72 Hz), 7.21-7.17 (1H, t, C-H₁₇, J = 7.32, 7.24 Hz), (1H, t, C-H₁₂, J = 8.04 Hz), 6.71 (1H, s, C-H₉), 6.58-6.56 (1H, dd, C-H₁₃, J = 1.24, 7.72 Hz), 6.54-6.52 (1H, d, C-H₁₁, J = 8.24 Hz), 6.43-6.41 (1H, d, N-H, J = 7.76 Hz), 4.75-4.71 (1H, t, C-H₇, J = 8.36 Hz), 2.76-2.70 (1H, m, C-H₂), 2.43-2.29 (2H, m, C-H₆), 1.83 (2H, m, C-H_{3,5}), 1.67-1.63 (1H, m, C₃-H), 1.23-1.21 (1H, m, C-H₅) and 1.51- 1.47 (2H, m, C-H₄). The ¹³C-NMR spectrum (100MHz, DMSO-d₆) of the L1 showed peaks at δ_C (ppm); 23.44, 28.50, 31.21 and 41.54 were assigned to (C₃), (C₄), (C₅) and (C₆), respectively. Chemical shifts for the (C₂) and (C₇) were observed at δ_C = 56.06 and 56.61 ppm. Peaks at 112.32, 115.43, 118.48 and 122.54 ppm, assigned to (C₉), (C₁₃), (C₁₁) and (C₁₀), respectively. Signals detected at 127.42, 127.93 and 128.69 ppm were assigned to (C₁₇), (C_{15,15}) and (C_{16,16}), respectively. The peak at 130.89 ppm is attributed to (C₁₂), while signals at 142.15 and 150.11 ppm are assigned to (C₁₄) and (C₈), respectively. The C=O of the carbonyl group appears at 211.29 ppm.

Synthesis of L2 and L3

The procedure used for the formation of L2 was similar to that mentioned for L1 using a similar amount of the starting materials, but *o*-bromoaniline (1.1ml, 10mmol) was employed in place of *m*-bromoaniline. Further, L3 was obtained in an analogous procedure to that of L1, but *p*-methyl cyclohexanone (1.23ml, 10mmol) was used in place of cyclohexanone. The compounds L2 and L3 were isolated using a similar technique to that for L1.

For L2; Yield: 1.67g (46%), m.p = 125-127°C. Elemental analysis: (C.H.N) Found, (Calc. %); C=63.74 (63.70), H= 5.74 (5.63), N=4.10 (3.91). FT-IR (KBr), 3387ν(N-H), 1703 ν(C=O), 1593cm⁻¹ ν(C=C)_{aromatic} and 1498 δ(N-H).

For L3; Yield: 1.50g (42%), m.p = 155-157°C.

Elemental analysis: (C.H.N) Found, (Calc. %); C=64.42 (64.51), H= 6.01 (5.90), N=3.87 (3.76). FT-IR(L3) (KBr), 3396ν(N-H), 1699 ν(C=O), 1596cm⁻¹ ν(C=C)_{aromatic} and 1512 δ(N-H).

NMR data of L2 and L3

The ¹H-NMR spectrum (400MHz, DMSO-d₆) of L2 showed peaks at δ_H (ppm); 7.42-7.40 (2H, d, C-H_{15,15}-, J = 7.24 Hz), 7.38-7.36 (1H, dd, C-H₁₀, J = 1.4, 7.88 Hz), 7.30-7.27 (1H, t, C-H_{16,16}-, J = 7.4, 7.72 Hz), 7.20-7.16 (1H, t, C-H₁₇, J = 7.32 Hz), 7.03-6.99 (1H, dt, C-H₁₁, J = 1.24, 1.28; 8.36 Hz), 6.64-6.55 (1H, d, C-H₁₃, J = 8.32 Hz), 5.55-5.53 (1H, d, N-H, J = 8.24 Hz), 6.48-6.44 (1H, dt, C-H₁₂, J = 1.32, 1.36; 7.8 Hz), and 4.80-4.76 (1H, t, C-H₇, J = 7.68, 7.76 Hz), 3.09-3.03 (1H, m, C-H₂). The multiplet at 2.43-2.36 and 2.31-2.26 ppm are assigned to (2H, m, C-H_{6a,b}). The recorded multiplet signals at 1.92-1.89, 1.82-1.80, 1.75-1.71 and 1.47-1.39 ppm that are equivalent to one proton each are assigned to (4H, m, C-H_{3a,b;5a,b}). The chemical shift that was recorded as a multiplet at 1.66-1.55 ppm has been assigned to (2H, m, C-H₄). The ¹³C-NMR spectrum (100MHz, DMSO-d₆) of the L2 showed peaks at δ_C (ppm); 23.91, 28.44, 32.22 and 42.10 were assigned to (C₃), (C₄), (C₅) and (C₆), respectively. Chemical shifts for the (C₂) and (C₇) were observed at 56.31 and 57.25 ppm, respectively. Resonances at 109.51, 113.10, 118.48 and 127.40 ppm, assigned to (C₉), (C₁₃), (C₁₁) and (C₁₇), respectively. Signals at 127.73, 128.69 and 128.85 ppm were assigned to (C_{15,15}), (C_{16,16}) and (C₁₂), respectively. Resonances at 142.04 and 144.65 ppm are assigned to (C₁₄) and (C₈), respectively. The C=O of the carbonyl group appears as estimated downfield at 212.44 ppm.

The NMR (¹H and ¹³C NMR) spectra of L3 indicated the presence of two isomers in the solution, the chair form (A) and the boat form (B), with a 9:1 ratio, respectively. The ¹H-NMR spectrum (400MHz, DMSO-d₆) of L3 showed peaks at δ_H (ppm); 7.36-7.34 (2H, d, C-H_{15,15}-, J = 8.32 Hz), 7.31-7.27 (2H, t, C-H_{16,16}-, J = 7.36, 7.76 Hz), 7.21-7.17 (1H, t, C-H₁₇, J = 7.20, 7.16 Hz), 6.90-6.86 (1H, t, C-H₁₂, J = 8.40, 8.0 Hz), 6.61 (1H, s, C-H₉). Peaks at 6.57-6.55 (1H, d, N-H, J = 7.80 Hz), 6.44-6.43 and (1H, d, C-H₁₁, J = 6.52 Hz), 6.41-6.40 (1H, d, C-H₁₃, J = 6.52 Hz), 4.58-4.55 (1H, t, C-H₇, J = 6.96 Hz), 2.96-2.89 (1H, p, C-H₂), 2.55-2.44 and 2.20-2.16 (2H, m, C-H₆) and (1H, m, C-H₄), respectively, 1.91-1.86 (2H, m, C-H₃), peaks at 1.48-1.45 and 1.26-1.19 and ppm were related to (1H, m, C-H_{5a}) and (1H, m, C-H_{5b}), respectively. The methyl group has been recorded as a doublet at 0.80-0.79 ppm with three protons integration (3H, d, Me, J = 6.4 Hz). The ¹³C-NMR spectrum (100MHz, DMSO-d₆) of L3 showed peaks at δ_C (ppm); 21.08, 31.32, 35.80, 39.10 and 41.52 assigned to (-Me), (C₃), (C₄), (C₅) and (C₆), respectively. Chemical shifts for the (C₂) and (C₇) were observed at 54.51 and 55.41 ppm, respectively. Resonances that were observed at 111.39, 114.53, 117.66, 122.06 and 126.86 were assigned to (C₉), (C₁₃), (C₁₁), (C₁₀) and (C₁₇), respectively. Signals at 127.36, 128.32 and 130.46

ppm were attributed to (C_{15,15'}), (C_{16,16'}) and (C₁₂), respectively. The resonances at 141.70 and 149.74 ppm are assigned to (C₁₄) and (C₈), respectively. The C=O of the carbonyl group appears as estimated downfield at δ_c = 210.04 ppm. The boat form recorded the following resonances at δ_c = 20.64, 31.31, 38.20, 39.31, 55.58, 56.17, 112.61, 115.62, 118.57, 127.16, 127.52, 128.18, 130.39, 141.54, 149.45 and 212.14 ppm.

Biological Activity

The well diffusion method was used to investigate the efficiency of the Mannich compounds against pathogenic bacteria under aerobic circumstances. The inhibitory activity against all pathogenic microorganisms was tested using Mueller-Hinton agar. After growing each microorganism in (*Escherichia coli*, *Klebsiella pneumoniae*, *Staphylococcus aureus* and *Bacillus subtilis*) in a nutrient broth, the agar plates were inoculated with (1.5 × 10⁸ (CFU)/ ml for bacteria in comparison to 0.5 McFarland tube. In the Mueller-Hinton agar plate, wells (6mm) were cut and 100 μ L of the tested compounds were added to each well. For bacteria, plates were incubated at 37°C for 24h. The diameter of inhibitory zones (mm) was used to assess activity [63]. For the fungi, potato dextrose agar was used as a nutrient. After growing the microorganism in potato dextrose broth (*Candida albicans*), agar plates were inoculated with 1.5 × 10⁶ (CFU)/ ml, wells (6mm) were cut and 100 μ L of Mannich bases were added to each well. The plates were incubated at

28°C for 72h. The diameter of inhibitory zones (mm) was used to assess the activity of the tested compounds.

3. Results and discussion

The formation of Mannich compounds (L1-L3), Fig. 1, was achieved via a one-pot multiple component reaction using ethanol solvent as the medium reaction and CaCl₂ as a catalyst. The reaction of benzaldehyde, *m*-bromoaniline with cyclohexanone or 4-methylcyclohexanone, in an equivalent mole ratio, resulted in the preparation of L1 and L3, respectively. The synthesis of L2 was derived from the reaction of benzaldehyde, *o*-bromoaniline and cyclohexanone. The title compounds are isolated in moderate yields as air-stable solids. The compounds are soluble completely in CHCl₃, benzene, DMSO and DMF solvents. The entity of the Mannich-bases was confirmed using physicochemical techniques. These include elemental analysis (Table 1) that, FT-IR (Table 2), UV-Vis, electrospray mass spectroscopy and ¹H- and ¹³C-NMR spectra. The obtained microanalyses data agree well with the calculated one.

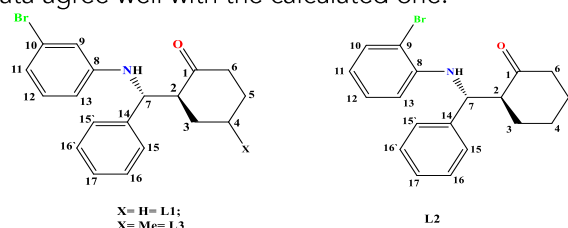


Fig. 1: Chemical structure of compounds (L1-L3).

Table 1: Microanalysis and physical properties of L1-L3.

Comp.	Molecular Formula	Yield %	m.p.°C	Colour	Micro-analysis; (calc.) found %		
					C	H	N
L1	C ₁₉ H ₂₀ NOBr	51	134-136	White Crystal	(63.70) 63.41	(5.63) 5.69	(3.91) 3.78
L2	C ₁₉ H ₂₀ NOBr	46	125-127	White Crystal	(63.70) 63.74	(5.63) 5.74	(3.91) 4.10
L3	C ₂₀ H ₂₂ NOBr	42	155-157	White Crystal	(64.51) 64.42	(5.90) 6.01	(3.76) 3.87

FT-IR spectra

The prominent infrared peaks of the Mannich bases (L1-L3) together with their assignments are listed in (Table 2). The FTIR spectra of the compounds, see Fig. 2, confirmed the formation of the title compounds. The spectra indicated a band at ca. 3385 cm⁻¹ assigned to the ν (NH) of the secondary amine of the Mannich bases [11]. The strong band that related to the ν (C=O) of the carbonyl group was observed at 1695, 1703 and 1699 cm⁻¹ in the spectra of the L1, L2 and L3, respectively [11, 12, 14].

Table 2: The FT-IR spectral data of HL and its complexes (cm⁻¹).

Comp.	ν (N-H)	ν (C-H) _{aro.}	ν (C-H) _{Al.}	ν (C=O)	ν (C=C)	δ (N-H)
L1	3382	3055	2943	1695	1602	1512
L2	3387	3059	2929	1703	1593	1496
L3	3396	3085	2954	1699	1596	1512

NMR spectra

The NMR (¹H- and ¹³C-NMR) spectra, which were acquired in DMSO-d₆ solvents, confirmed the presence of the required numbers of the nuclei of the isolated compounds (see experimental section).

Further, the NMR data confirmed the purity of the prepared Mannich compounds (L1-L3). The NMR spectra indicated two sets of chemical shifts that are allocated at the aromatic and aliphatic regions. The ¹H-NMR spectra of the Mannich bases (L1-L3) are collected in Fig. 3. The spectra indicated a doublet peak between 6.43-6.41, 5.55-5.53 and 6.57-6.55 ppm for L1, L2 and L3, respectively. This signal is equivalent to one proton, which is assigned to the (N-H) group. The chemical shifts that appeared between 4.75-4.71, 4.80-4.76 and 4.58-4.55 ppm for L1, L2 and L3, respectively were assigned to C₇-H. This peak was recorded, as expected, as a triplet with one proton integration. Further, the spectrum of L3 indicated a doublet equivalent to three protons attributed to the methyl group that attached to the cyclohexanone moiety. The spectra of L1 and L2 indicated the presence of one isomer on the NMR time scale. However, the spectrum of L3 confirms the presence of two isomers with a 9:1 ratio. The isomer with the high ratio is attributed to the chair form (isomer A) and the other one represents the boat form (isomer B), Fig. 4. The ¹³C-NMR spectra of L1-L3 in DMSO-d₆ solvents are collected in Fig. 5. The

spectra indicated two sets of resonances in the aliphatic and aromatic area. The spectra revealed chemical shift at 211.29, 212.44 and 210.40 ppm assigned to the C=O of the carbonyl group of L1, L2 and L3, respectively. More, the spectrum of L3

indicated the presence of another small signal at 212.14 ppm and a set of small peaks beside the main ones. This is due to the presence of two conformational isomers in solutions (the chair and the boat, Fig. 4).

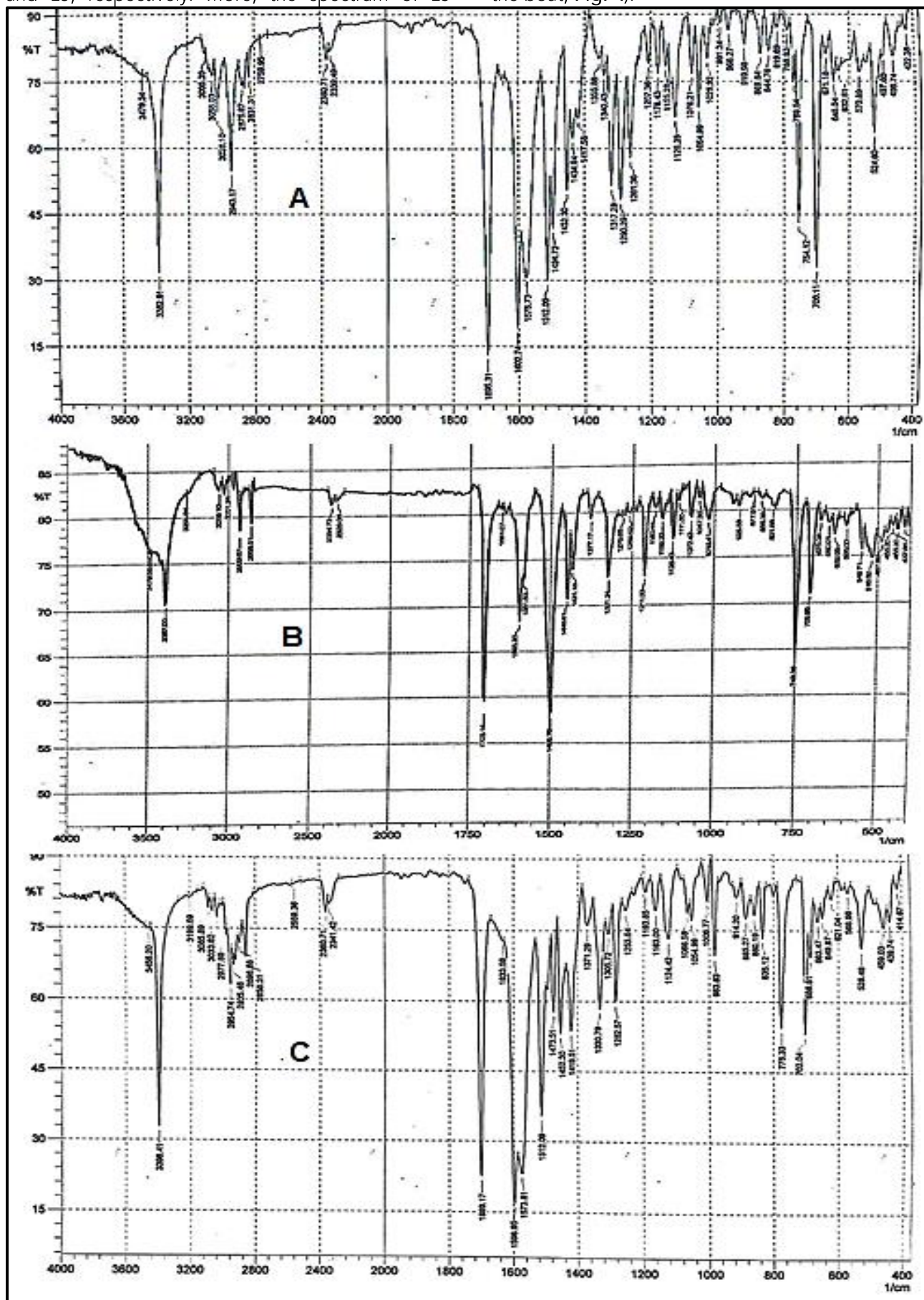


Fig. 2: FT-IR spectra of; (A) L1, (B) L2 and (C) L3.

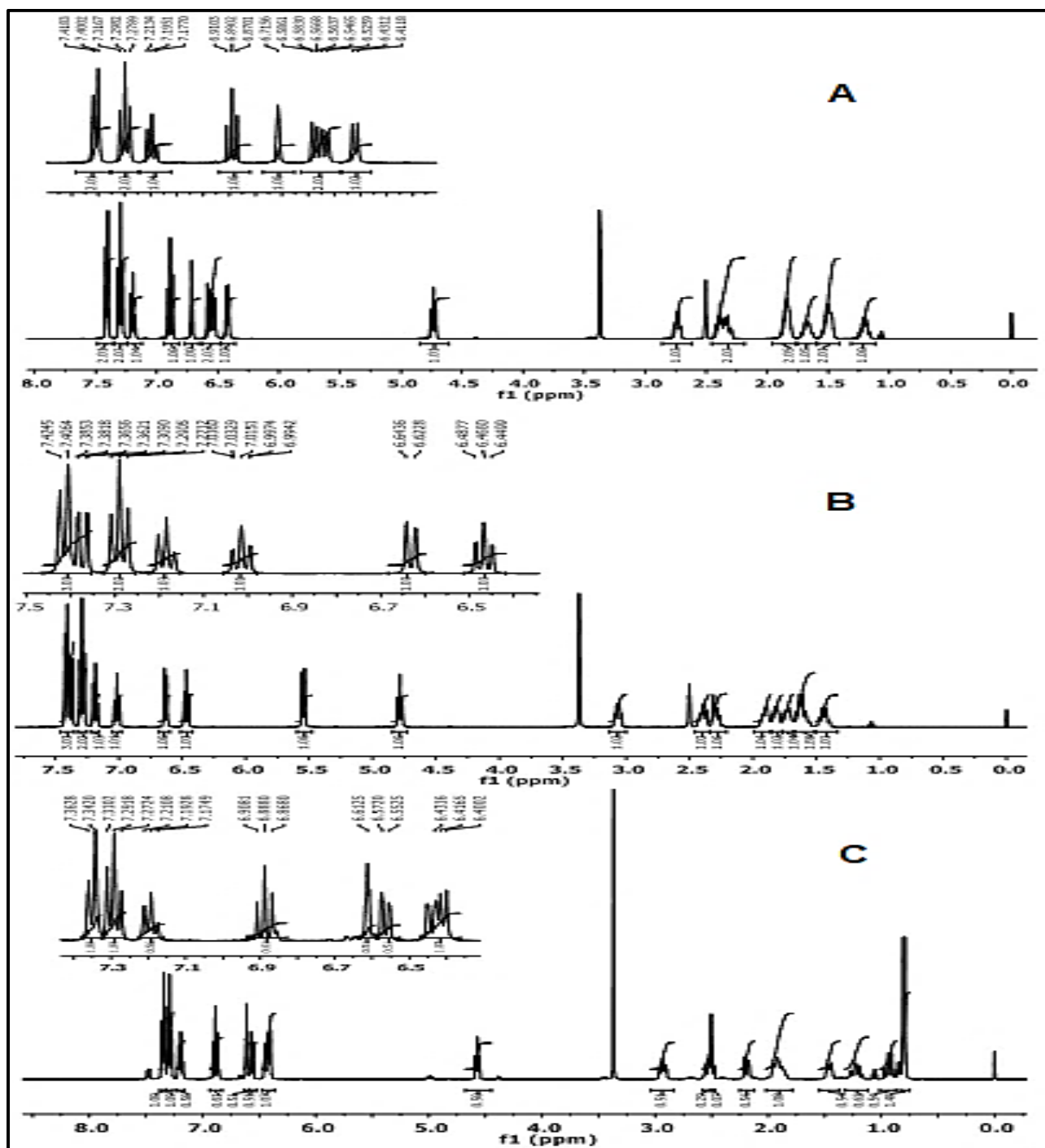


Fig. 3: ^1H NMR spectra in $\text{DMSO}-d_6$ solutions of; (A) = L1, (B)= L2 and (C)= L3.

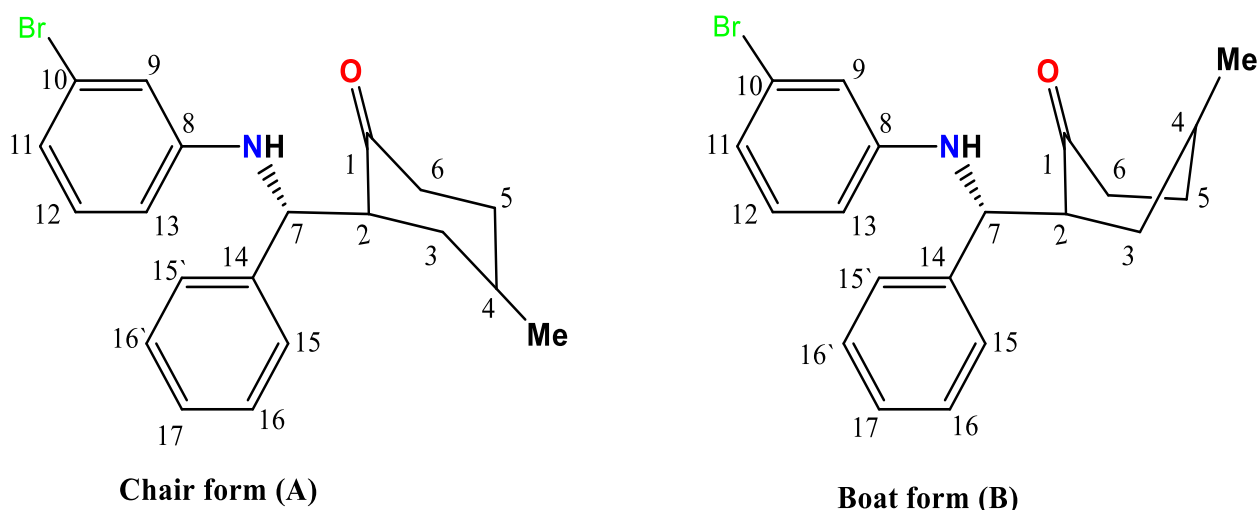


Fig. 4: The boat and chair conformations of L3 in $\text{DMSO}-d_6$ solution.

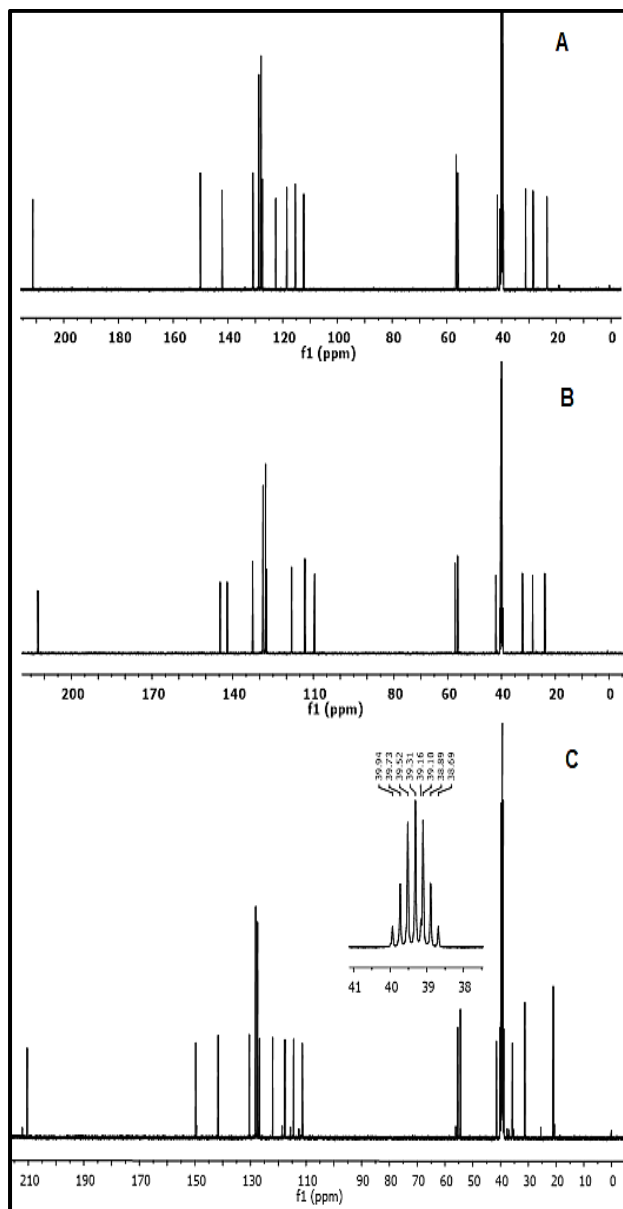


Fig. 5: ^{13}C NMR spectra in $\text{DMSO}-d_6$ solutions of; (A) = L1, (B)= L2 and (C)= L3.

Mass spectra

The electrospray (+) mass spectrum of L1, Fig. 6, a peak at $m/z = 394.4$ amu (4 %). This peak is attributed to $(\text{M} + (2\text{H}_2\text{O}) + \text{H})^+$, which requires 394.10 amu calculated for $\text{C}_{19}\text{H}_{25}\text{BrNO}_3$. The fragment at $m/z = 359.4$ amu (27 %) attributed to $(\text{M} + 2\text{H})^+$, which requires 359.1 amu, calculated for $\text{C}_{19}\text{H}_{22}\text{BrNO}$. The successive fragments at 261.8 (100 %, basic peak), 180.02 (51 %) and 151.70 (12 %) are related to $[\text{M} - \{(2\text{H}_2\text{O}) + \text{H} + (\text{C}_6\text{H}_{10})\}]^+$, $[\text{M} - \{(2\text{H}_2\text{O}) + \text{H} + (\text{C}_6\text{H}_{10})\} + (\text{HBr})]^+$ and $[\text{M} - \{(2\text{H}_2\text{O}) + \text{H} + (\text{C}_6\text{H}_{10})\}]^+$, $[\text{M} - \{(2\text{H}_2\text{O}) + \text{H} + (\text{C}_6\text{H}_{10})\} + (\text{HBr}) + (\text{H}_2\text{C}=\text{NH})]^+$, respectively. Fragments recorded at 129.3 (20 %), 115.1 (21 %), 91.1 (42 %), 77.2 (20 %) and 55.1 (16 %) amu are correlated to $[\text{M} - \{(2\text{H}_2\text{O}) + \text{H} + (\text{C}_6\text{H}_{10})\} + (\text{HBr}) + (\text{HCC}-\text{CH}_2-\text{CN})]^+$, $[\text{M} - \{(2\text{H}_2\text{O}) + \text{H} + (\text{C}_6\text{H}_{10})\} + (\text{HBr}) + (\text{HCCH} + \text{HCC}-\text{CH}_2)]^+$, $[\text{M} - \{(2\text{H}_2\text{O}) + \text{H} + (\text{C}_6\text{H}_{10})\} + (\text{HBr}) + (\text{HN}=\text{C}=\text{C}=\text{C}=\text{HC}-\text{CCH})]^+$, $[\text{M} - (\text{C}_4\text{H}_2) + (\text{HBr})] + (\text{CHCH}) + (\text{CH}_2=\text{C}=\text{CH}_2)^+$, $[\text{M} - \{(2\text{H}_2\text{O}) + \text{H} + (\text{C}_6\text{H}_{10})\} + (\text{HBr}) + (\text{CH}_3\text{N}=\text{C}=\text{C}=\text{C}=\text{HC}-\text{CCH})]^+$ and $[\text{M} - \{(2\text{H}_2\text{O}) + \text{H} + (\text{C}_6\text{H}_{10})\} + (\text{HBr}) + (\text{CH}_3\text{N}=\text{C}=\text{C}=\text{C}=\text{HC}-\text{CCH}) + (\text{HCCH})]^+$, respectively.

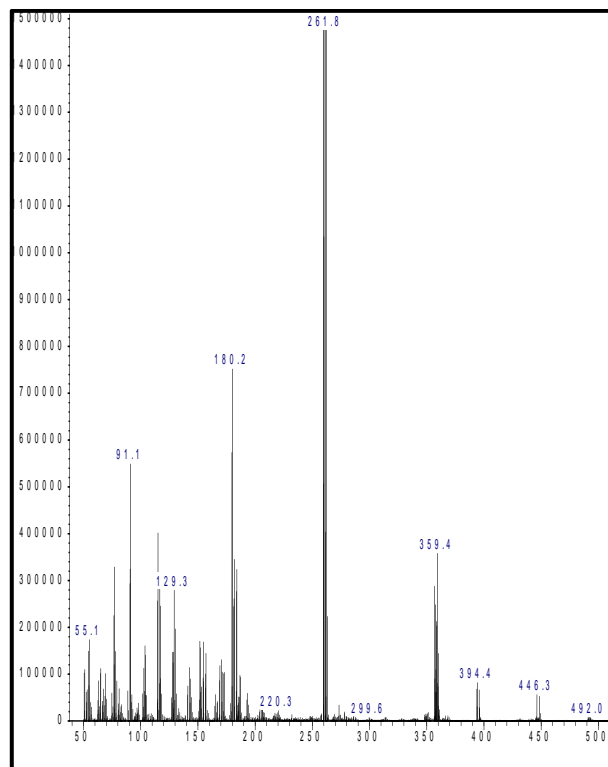


Fig. 6: The electrospray (+) mass spectrum of L1.

The electrospray (+) mass spectrum of L2, Fig. 7, shows a peak at $m/z = 394.10$ (8 %) amu, attributed to $(\text{M} + (2\text{H}_2\text{O}) + \text{H})^+$, requires = 394.10 amu calculated for $\text{C}_{19}\text{H}_{25}\text{BrNO}_3$. The parent ion peak at $m/z = 356.90$ amu (17 %). This peak is attributed to $(\text{M})^+$, which requires 357.07 amu calculated for $\text{C}_{19}\text{H}_{20}\text{NBrNO}$. Fragmentations detected at $m/z = 262.10$ (3100 %, basic peak), 181.10 (28 %) and 154.90 (20 %) are related to $[\text{M} - (\text{C}_4\text{H}_2)]^+$, $[\text{M} - (\text{C}_4\text{H}_2) + (\text{HBr})]^+$ and $[\text{M} - (\text{C}_4\text{H}_2) + (\text{HBr})] + (\text{CHCH})^+$, respectively. Peaks recorded at 129 (20 %), 115.1 (21 %), 91.1 (42 %), 77.1 (20 %) and 55.1 (16 %) amu are correlated to $[\text{M} - (\text{C}_4\text{H}_2) + (\text{HBr})] + (\text{CHCH}) + (\text{CH}_4)^+$, $[\text{M} - (\text{C}_4\text{H}_2) + (\text{HBr})] + (\text{CHCH}) + (\text{CH}_2=\text{C}=\text{CH}_2)^+$, $[\text{M} - (\text{C}_4\text{H}_2) + (\text{HBr}) + (\text{CHCH}) + (\text{HC}=\text{N}=\text{C}=\text{C}=\text{CH})]^+$, $[\text{M} - (\text{C}_4\text{H}_2) + (\text{HBr}) + (\text{CHCH}) + (\text{CH}_3\text{C}=\text{N}=\text{C}=\text{C}=\text{CH})]^+$, and $[\text{M} - (\text{C}_4\text{H}_2) + (\text{HBr}) + (\text{CHCH}) + (\text{CH}_3\text{C}=\text{N}=\text{C}=\text{C}=\text{CH})]^+$, respectively.

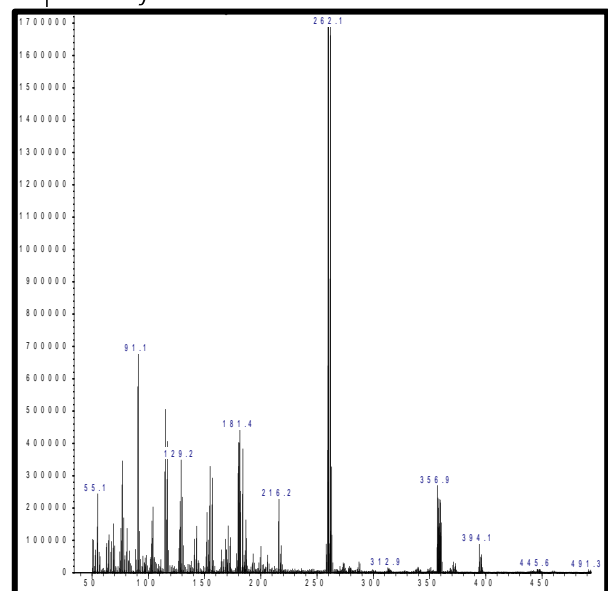


Fig. 7: The electrospray (+) mass spectrum of L2.

The electrospray (+) mass spectrum of L3, Fig. 8, shows the parent ion peak at $m/z = 370.7$ amu (19 %). This peak is attributed to $(M)^+$, which requires 371.08 amu calculated for $C_{20}H_{22}NBrNO$. Peaks detected at $m/z = 326.90$ (3 %), 287.30 (5 %), 261.70 (100 %, basic peak), 181.10 (29 %) and 154.90 (22 %) are related to $[M-(CH_3CHO)]^+$, $[M-(CH_3CHO)+(CH_2=C=CH_2)]^+$, $[M-(CH_3CHO)+(CH_2=C=CH_2)+(CHCH)]^+$, $[M-(CH_3CHO)+(CH_2=C=CH_2)+$ and $[M-$

$(CH_3CHO)+(CH_2=C=CH_2)+(CHCH)]^+(HBr)+$ $(CHCH)^+$, respectively. Peaks detected at 129 (19 %), 91.1 (42 %) and 55.1 (27 %) amu are correlated to $[M-(CH_3CHO)+(CH_2=C=CH_2)+(CHCH)]^+(HBr)+(CHCH)^+$, $[M-(CH_3CHO)+(CH_2=C=CH_2)+(CHCH)]^+(HBr)+(CHCH)^+$ and $[M-(CH_3CHO)+(CH_2=C=CH_2)+(CHCH)]^+(HBr)+(CHCH)^+$ and $[M-(CH_3CHO)+(CH_2=C=CH_2)+(CHCH)]^+(HBr)+(CHCH)^+$, respectively.

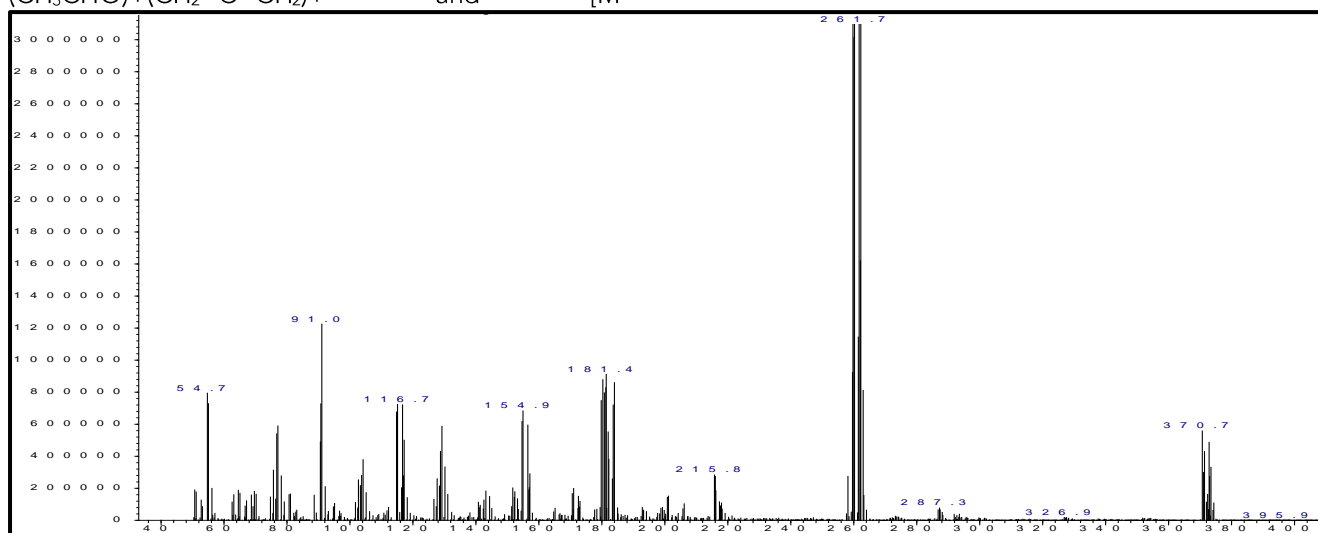


Fig. 8: The electrospray (+) mass spectrum of L3.

Electronic spectra

The electronic spectra of L1-L3 in DMSO solutions are presented in Fig. 9. The spectra of L1 and L2 indicated peaks at 236 nm (42373cm^{-1} , $\epsilon_{\text{max}} = 1347\text{molar}^{-1}\text{cm}^{-1}$), 307 nm (32573cm^{-1} , $\epsilon_{\text{max}} = 1634\text{molar}^{-1}\text{cm}^{-1}$) and 234 nm (42735cm^{-1} , $\epsilon_{\text{max}} = 2428\text{molar}^{-1}\text{cm}^{-1}$), 303 nm (33003cm^{-1} , $\epsilon_{\text{max}} = 760\text{molar}^{-1}\text{cm}^{-1}$) for L1 and L2, respectively. These peaks were assigned

to the ligand field transitions ($\pi \rightarrow \pi^*$ and $n \rightarrow \pi^*$) [7,8]. The spectrum of L3 indicated peaks at 257 nm (38911cm^{-1} , $\epsilon_{\text{max}} = 1878\text{molar}^{-1}\text{cm}^{-1}$), 286 nm (34965cm^{-1} , $\epsilon_{\text{max}} = 1613\text{molar}^{-1}\text{cm}^{-1}$) and 308 nm (32468cm^{-1} , $\epsilon_{\text{max}} = 548\text{molar}^{-1}\text{cm}^{-1}$). These electronic data are attributed to the ligand field ($\pi \rightarrow \pi^*$ and $n \rightarrow \pi^*$) [7,8].

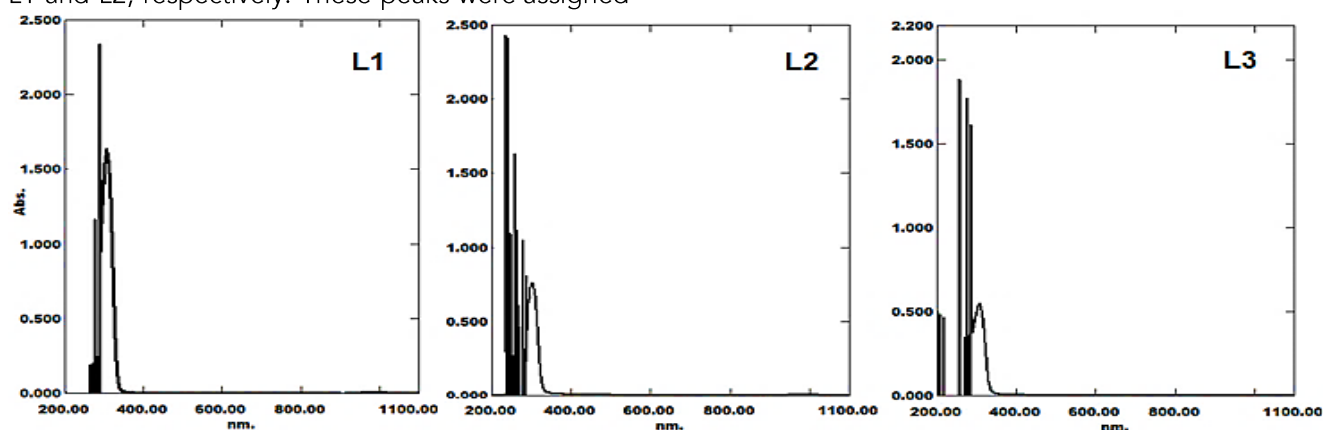


Fig. 9: The electronic spectra of L1-L3 in DMSO solutions.

Biological activity

The synthesized compounds (L1-L3) were examined against, four types of bacteria, *Staphylococcus aureus* and *Bacillus subtilis* (G-positive) and *Escherichia coli* and *Klebsiella pneumonia* (G-negative) and the fungi species *Candida albicans*. The observed activity was expressed in terms of a millimetre (mm). This was based on the measuring of the inhibition zone diameters and correlated with the DMSO solvent that was used as a control, which

showed no activity against the bacterial strains and fungi species [8,9]. The antibiotics Ceftriaxone and Fluconazole were introduced as reference drugs for bacteria and fungi species, respectively. The tested compounds indicated different antimicrobial activity against the examined bacteria. In general, the tested compounds indicated the highest activity against the G-positive strain. More, the referenced drug indicated higher activity, compared with the examined compounds, see Table 3 and Fig. 10. The anti-fungal data of the tested compounds indicated

a higher activity for these compounds, compared with Fluconazole (Table 3 and Fig. 10).

Comp.	Inhibition zones (mm)				
	Bacterial strains				Fungi species
	<i>Staphy. aureus</i>	<i>Bacil. subtilis</i>	<i>Esch. coli</i>	<i>Kleb. pneumonia</i>	<i>Candida albicans</i>
DMSO	-	-	-	-	-
Ceftriaxone	30	32	30	31	-
Fluconazole	-	-	-	-	15
L1	23	18	15	16	19
L2	22	17	13	13	21
L3	16	19	14	15	20

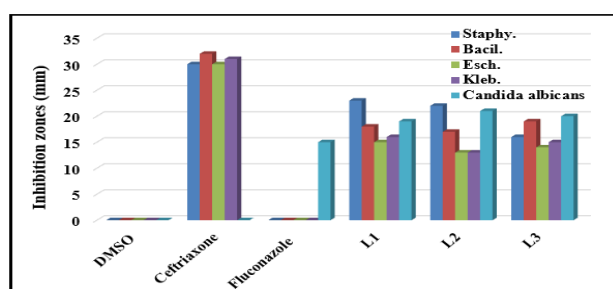


Fig. 10: The inhibition zone diameter (mm) for compounds against bacteria and fungal species.

4. Conclusions

The formation and structural characterisation of three Mannich β -aminocarbonyl compounds (L1-L3) are presented in this publication. The synthesis of these compounds was based on a one-pot reaction using CaCl_2 as a catalyst. The mixing of benzaldehyde and *m*-bromoaniline with cyclohexanone or 4-methylcyclohexanone in an equivalent mole ratio resulted in the preparation of L1 and L3, respectively. The synthesis of L2 was derived from the reaction of an equimolar ratio of benzaldehyde, *o*-bromoaniline and cyclohexanone. The entity of the isolated compounds was confirmed using a range of physicochemical techniques. The FTIR for the title compounds revealed bands characteristic for the secondary amine and the carbonyl moiety. The ESMS indicated the parent ion peaks of the isolated bases. The NMR analyses confirmed the corrected number with the expected chemical shifts of the nucleus. Further, the NMR data of L3 indicated the presence of two isomers in solutions (the chair and the boat with a 9:1 ratio, respectively) on the NMR time scale.

Acknowledgements

We are grateful to the University of Baghdad and the College of Education for Pure Science (Ibn Al-Haitham) for providing Ms AME with the PhD studentship and lab facilities.

References

João F. Allochio Filho, Bárbara C. Lemos, Acácio S. de Souza, Sergio Pinheiro, Sandro J. Greco,

Multicomponent Mannich reactions: General aspects, methodologies and applications, *Tetrahedron*, **73**, 50, 6977-7004, (2017).

Baidaa K. Al-Rubaye, Alice Brink, Gary J. Miller, Herman Potgieter and Mohamad J. Al-Jeboori, Crystal structure of (E)-4-benzylidene-6-phenyl-1,2,3,4,7,8,9,10-octahydrophenanthridine", *Acta Crystallog. E* **73**, 1092-1096, (2017).

Baidaa K. Al-Rubaye, Herman Potgieter and Mohamad J. Al-Jeboori, "An Efficient One-Pot Approach for the Formation of Phenanthridine Derivative; Synthesis and Spectral Characterisation", *Der Chemica Sinica*, **8**(3), 365-370, (2017).

Talib H. Mawat and Mohamad J. Al-Jeboori, Synthesis and Spectral Characterisation of New β -Aminoketone Compounds, *Biochem. Cell. Arch.*, **19**(2), 4573-4580, (2019).

Jakub Iwanejko, Elżbieta Wojaczyńska, Tomasz K. Olszewski, Green chemistry and catalysis in Mannich reaction, *Current Opinion in Green and Sustainable Chemistry*, **10**, 27-34, (2018).

Gheorghe Roman, Mannich bases in medicinal chemistry and drug design, *European Journal of Medicinal Chemistry*, **89**, 743-816, (2015).

Talib H. Mawat and Mohamad J. Al-Jeboori, "Synthesis, characterisation, thermal properties and biological activity of coordination compounds of novel selenosemicarbazone ligands", *Journal of Molecular Structure*, **1208**, 127867, (2020).

Safaudeen A. Hussain and Mohamad J. Al-Jeboori, "New Metal Complexes Derived from Mannich-Base Ligand; Synthesis, Spectral Characterisation and Biological Activity", *Journal of Global Pharma Technology*, **11**(2), 548-560, (2019).

Ammar H. Al-Qazzaz and Mohamad J. Al-Jeboori, "New metal complexes derived from Mannich ligands; synthesis, spectral investigation and biological activity", *Biochemical and Cellular Archives*, **20**, Supplement 2, 4207-4216, (2020).

Mohamad J. Al-Jeboori, Fahad A. Al-Jebouri and Muayed A. R. Al-Azzawi, "Metal complexes of a new class of polydentate Mannich bases; synthesis and spectroscopic Characterisation", *Inorganica Chimica Acta*, **379**, 163–170, (2011).

Mohamad J. Al-Jeboori, Mahmoud S. Al-Fahdawi and Ausama A. Sameh, "New homoleptic metal complexes of Schiff-bases derived from 2,4-dip-tolyl-3-azabicyclo[3.3.1]nonan-9-one", *Journal of Coordination Chemistry*, Vol. **62**, Issue 23, 3853, (2009).

Ahlam J. Abdul-Ghani, Mohamad J. Al-Jeboori and Ahmed Jasim M. Al-Karawi, "Synthesis and characterisation of new N_2S_2 and N_2O_2 Mannich base ligands derived from phosphinic acid and their metal complexes", *Journal of Coordination Chemistry*, Vol. **62**, Issue 16, 2736, (2009).

Talib H. Mawat and Mohamad J. Al-Jeboori, "Novel Metal Complexes Derived from Selenosemicarbazone Ligand; Synthesis, Spectral Investigation and Biological Activity", *Journal of Global Pharma Technology*, **11**(09), (Suppl.), 126-138, (2019).